EBioMedicine 30 (2018) 94–104

Contents lists available at ScienceDirect

EBioMedicine

journal homepage: www.ebiomedicine.com

Research Paper

Oligodendrocyte Progenitor Cells and Macrophages/Microglia Produce Glioma Stem Cell Niches at the Tumor Border

Takuichiro Hide [a,*,1], Yoshihiro Komohara [b], Yuko Miyasato [b], Hideo Nakamura [a], Keishi Makino [a], Motohiro Takeya [b], Jun-ichi Kuratsu [a], Akitake Mukasa [a], Shigetoshi Yano [a]

[a] Department of Neurosurgery, Graduate School of Life Sciences, Kumamoto University, Japan
[b] Department of Cell Pathology, Graduate School of Life Sciences, Kumamoto University, Japan

ARTICLE INFO

Article history:
Received 18 August 2017
Received in revised form 19 February 2018
Accepted 28 February 2018
Available online 1 March 2018

Keywords:
Oligodendrocyte progenitor cell
Macrophage
Microglia
Stemness
Chemoradioresistance
Recurrence
Border niche
Glioblastoma
Glioma stem cells niche
microRNA

ABSTRACT

Glioblastoma (GBM) usually develops in adult brain white matter. Even after complete resection, GBM recurs around the tumor removal cavity, where GBM cells acquire chemo-radioresistance. Characterization of the tumor border microenvironment is critical for improving prognosis in patients with GBM. Here, we compared microRNA (miRNA) expression in samples from the tumor, tumor border, and periphery by miRNA microarray. The top three of miRNAs showing higher expression in the tumor border were related to oligodendrocyte differentiation, and pathologically oligodendrocyte lineage cells were increased in the border, where macrophages and microglia also colocalized. Medium cultured with oligodendrocyte progenitor cells (OPCs) and macrophages induced stemness and chemo-radioresistance in GBM cells, similar to that produced by FGF1, EGF and HB-EGF, IL-1β, corresponding to OPCs and macrophages, respectively. Thus, OPCs and macrophages/microglia may form a glioma stem cell niche at the tumor border, representing a promising target for prevention of recurrence.

1. Introduction

Glioblastoma (GBM) shows rapid growth and invasion; thus, standard treatment, including maximum resection of the tumor mass plus chemo-radiotherapy (temozolomide [TMZ] and radiation [60 Gy]) is performed immediately. However, the mean 5-year survival rate is still <10% (Stupp et al., 2009). Studies focusing on glioma stem cells (GSCs) and big data from microarray analysis and next-generation sequencing have helped to elucidate some of the mechanisms of GBM development and recurrence (Singh et al., 2004; Sturm et al., 2012). However, further advancements are needed to improve patient prognosis.

Generally, GBM cells start to invade into the white matter even during the early stage of tumor development and in some cases can extend into the contralateral hemisphere through the corpus callosum (Wilson, 1992). The tumor mass of GBM can be detected in gadolinium-enhanced T1-weighed images (Gd-T1WI) from magnetic resonance imaging (MRI) because of leakage of contrast-enhancing reagent from the abnormal tumor vessels, where the blood-brain-barrier is broken (Liu et al., 2016). Moreover, GBM is typically surrounded by large edema in the white matter, which can be detected in low- and high-intensity areas in T1WI and T2WI, and where invading GBM cells are detected pathologically. Although enhanced lesions and edematous areas can be completely eliminated by intensive treatment, GBMs usually recur in the white matter around the tumor removal cavity. Radiation is applied 2–3 cm beyond the primary enhanced lesion in Gd-T1WI, and approximately 78.5% of recurrent GBMs are found around the primary lesion (inside and at the margin of the radiation field: 72.2% and 6.3%, respectively) (Brandes et al., 2009), suggesting that that GSCs survive in GSC niches at the border of the enhanced lesion (Hide et al., 2013). To date, although intratumoral hypoxic niches and perivascular niches have been reported, niches outside of the tumor mass have not been frequently observed (Charles et al., 2011; Fidoamore et al., 2016; Hide et al., 2013; Ishii et al., 2016; Quail and Joyce, 2017). For the growth of GBM, glioma cells as well as immune cells, neural cells, brain vascular cells, and extracellular matrix are essential (Quail and Joyce, 2017). Determination of the specific microenvironment required for chemo-radioresistance and local recurrence is fundamental for improving the overall survival and quality of life of patients with GBM.

Accordingly, in this study, we hypothesized that some molecules at this border area (tumor-brain interface) may enhance chemo-radioresistance and recurrence by promoting the stem cell

* Corresponding author at: 1-15-1 Kitasato, Minami-ku, Sagamihara 252-0374, Japan.
E-mail address: thide@med.kitasato-u.ac.jp (T. Hide).
[1] Lead Contact.

https://doi.org/10.1016/j.ebiom.2018.02.024

characteristics of GBM cells. We focused on microRNAs (miRNAs) because of their unique features, including their regulation of multiple targets, secretion into the extracellular space, and function as communicators between tumor cells and the tumor microenvironment (Kohlhapp et al., 2015; Kros et al., 2015; Li et al., 2016). Indeed, analysis of the expression profiles of miRNAs in the border area of the tumor mass may provide essential information regarding the most suitable microenvironment for GSCs, i.e., the GSC niche, and functional characterization of this microenvironment may contribute to the development of new GBM treatment strategies.

2. Materials and Methods

2.1. Evaluation of MRI Findings after Operation

Eighty-nine patients who were newly diagnosed with GBM from January 2013 to December 2015 were enrolled in this retrospective MRI study. Clinical data for patients with GBM were obtained at Kumamoto University Hospital with the patients' consent and in accordance with the guidelines of the Research Ethics Committee.

Complete resection was defined as a case where the enhanced mass lesion was completely deleted in Gd-T1WIs, acquired within 72 h after operation. Although enhanced lesions were completely removed, cases showing other residual suspicious mass lesions in MRI were classified in the partial resection group. Biopsy cases were also counted in the partial resection group. During the monthly MRI examination, initial recurrence was defined as the occurrence of new lesions in Gd-T1WIs in the complete resection group. The site of recurrence was classified into white matter, gray matter, and cerebrospinal fluid dissemination. Local recurrence indicated the emergence of new enhanced lesions at the area attached to the tumor removal cavity. Cerebrospinal fluid dissemination was considered distant recurrence.

2.2. Tissue Samples, Purification of RNAs, and miRNA Microarray

From the resected tissue, samples from three sites (intratumor tissue [tumor], just around the tumor mass [border], and peripheral area far from the tumor mass [periphery]) were obtained at Kumamoto University Hospital with the patients' consent and in accordance with the guidelines of the Research Ethics Committee. Each tissue sample was divided into two parts; one half was used for pathological examination while the other was frozen. RNA was then isolated from the frozen tissue using an miRNeasy Mini Kit (Qiagen, Hilden, Germany) after confirmation of pathological features. miRNA microarray analysis was then performed using the human miRNA Microarray Release 16.0, 8 × 60K kit (Agilent Technologies, Santa Clara, CA, USA),ordered from Hokkaido System Science Co., Ltd. (Sapporo, Japan). The samples were also routinely fixed in 10% neutral buffered formalin and embedded in paraffin (FFPE) for use in standard pathological examinations. miRNA expression data were deposited at the NCBI Gene Expression Omnibus (GEO) under the accession number GSE 109628.

2.3. miRNA In Situ Hybridization (ISH)

To confirm *miR-219-5p* expression in GBM samples and brain tissues from the xenograft mouse model, miRNA ISH was performed on 4-μm-thick FFPE sections. We used a miRCURY LNA microRNA ISH Optimization Kit (FFPE) (Exiqon, Vedbaek, Denmark), an LNA U6 snRNA probe as a positive control, and a miR-Scrambled LNA probe as a negative control. Additionally, *miR-21* (product code 90002) was used as a positive control for GBM tissue (Fig. S2B). To determine the appropriate conditions, ISH using *miR-219-5p* (miRCURY LNA Detection probe, 5′-DIG- and 3′-DIG-labeled *hsa-miR-219-5p*; Exiqon; product no. 204780) was performed in accordance with the manufacturer's protocol. Probes were hybridized at 55 °C for 60 min.

2.4. Immunohistochemistry

Tumor tissues were fixed in formalin overnight, embedded in paraffin, and then cut into 4-μm-thick sections. The following antibodies were used to detect antigens: rabbit anti-GFAP (1:2000; Dako), rabbit anti-Olig2 (1:100; Biocare Medical), rabbit anti-NG2 (1:200, Cell Signaling Technology, Danvers, MA, USA; and 1:2, hybridoma supernatant, American Type Culture Collection [ATCC], Manassas, VA, USA), O4 (1:2; hybridoma supernatant; ATCC), MBP (1:400 Nichirei), rabbit anti-Iba1 (1:2000; Medical Biological Laboratories), rabbit anti-Iba-1 antibody (Wako, Tokyo, Japan), anti-CD163 (1:200, 10D6, Novocastra, Newcastle, UK). Reactions were visualized using a diaminobenzidine substrate system (Nichirei). Two investigators, who were blinded to any information about the samples, evaluated the results. In immunofluorescent staining, the antibodies were detected using goat anti-rabbit IgG-A488 (1:400; Molecular Probes, Eugene, OR, USA) or goat anti-mouse IgG-Cy3 (1: 400; Jackson ImmunoResearch). All nuclei were counterstained with DAPI (1:1000; Wako).

2.5. GBM Cell Lines and Human GSCs

The human glioblastoma cell lines A172 and T98G were obtained from ATCC. A172 and T98G cells were cultured in Dulbecco's modified Eagle's medium (DMEM)/F-12 medium (Sigma Aldrich, St. Louis, MO, USA) supplemented with 10% fetal bovine serum (Nichirei) and 1% penicillin/streptomycin/amphotericin (Nacalai Tesque, Kyoto, Japan).

To establish human GSCs, samples from human GBMs were dissociated with the Papain Dissociation System (Worthington Biochemical Corporation, Lakewood, NJ, USA). After filtration, dissociated cells were cultured in serum-free medium with growth factors as previously described (Anai et al., 2014; Singh et al., 2004). All cells were incubated at 37 °C in an atmosphere containing 5% CO_2. To confirm their tumor-forming potential, 1×10^5 GSCs were injected into the brains of 8-week-old female ICR-nu mice (Crlj:CD1-Foxn1^{nu}; Charles River Japan) after anesthesia. Four weeks later, xenograft tumors had formed in the brain. Pathologically, the tumors showed high cellularity and necrosis similar to that of the original tumor (Fig. 3A and B).

2.6. Cell Culture and Preparation of CM

T98G and A172 cell lines were obtained from ATCC and cultured in DMEM/F-12 supplemented with 10% FBS and penicillin/streptomycin (Wako). CM from the two glioma cell lines was collected, and cells were cultured in DMEM/F-12 supplemented with 10% FBS and penicillin/streptomycin for 2 days (CM-A172 and CM-T98G).

Human OPCs were obtained from ScienCell Research Laboratories (cat. #1610; ScienCell Research Laboratories, Carlsbad, CA, USA) and cultured with Oligodendrocyte Precursor Cell Medium (cat. #1601; ScienCell Research Laboratories). For the preparation of CM from oligodendrocytes, cells were washed with serum-free DMEM/F-12 and cultured in DMEM/F-12 supplemented with 10% FBS and penicillin/streptomycin for 2 days, and supernatants were then collected as CM-OPC.

Peripheral blood mononuclear cells were obtained from healthy volunteer donors, all of whom had provided written informed consent for the use of their cells in accordance with the study protocols approved by the Kumamoto University Hospital Review Board (#1169).

$CD14^+$ monocytes were isolated using CD14-microbeads (Miltenyi Biotec, Bergisch Gladbach, Germany). These monocytes were plated in 12-well culture plates (2×10^5 cells/well; UpCELL, CellSeed, Tokyo, Japan) and cultured in 2% human serum, 1 ng/mL granulocyte macrophage-colony stimulating factor (Wako), and 50 ng/mL macrophage-colony stimulating factor (Wako) for 7 days to induce macrophage differentiation. For preparation of CM from macrophages, cells were washed with serum-free DMEM/F-12 and cultured in DMEM/F-12 supplemented with 10% FBS and penicillin/streptomycin for 2 days, and supernatants were then collected as CM-Mac.

2.7. Colony-Forming Assays

Cell lines (100 cells/50 μL/well) were cultured in DMEM/F-12 supplemented with 10% FBS and SphereMax (Wako) using a 96-well ultra-low attachment plate (Corning, NY, USA) for 10 days. CM (25 μL) was added to each well. The number of colonies (size > 100 μm) was counted under a microscope, and the total cell viability was evaluated by analyzing cellular ATP activity using a Cell Titer-Glo Luminescent Cell Viability Assay Kit (Promega, Madison, WI, USA).

Recombinant OPN, HB-EGF, OSM, GRO-a, IL-6, CCL1 (I309), TNF-α, IL-1β, C5a, IGF-II, IGF-BP3, FGF1, VEGF-C, PIGF1, EFEMP1, and EGF were purchased from Peprotech (Rocky Hill, NJ, USA), Wako, or R&D Systems (Minneapolis, MN, USA), and all cytokines were added at a final concentration of 10 ng/mL.

2.8. Real-Time Quantitative PCR (RT-qPCR)

Total RNA was isolated using an RNAiso Plus (Takara Bio Inc., Otsu, Japan). RNA was reverse-transcribed using a PrimeScript RT Reagent Kit (Takara Bio Inc.). Quantitative real-time PCR was performed using TaqMan polymerase with SYBR Green Fluorescence (Takara Bio Inc.) and an ABI PRISM 7300 Sequence Detector (Applied Biosystems, Foster City, CA, USA). The relative expression level was determined using the $2^{-\Delta\Delta Cq}$ normalization method. Predesigned primer sets for *Nanog*, *Sox2*, *ALDH1*, *Oct3/4*, *Bmi1*, and *ABCG2* were purchased from Takara Bio Inc. (Perfect Real Time PCR support system).

2.9. Western Blot Analysis

Cells were lysed in ice-cold lysis buffer (50 mM Tris, pH 8.0, 1 mM ethylenediaminetetraacetic acid, 150 mM NaCl, 1% NP-40) containing phosphatase inhibitor cocktail (R&D Systems) and protease inhibitor cocktail (Sigma-Aldrich, St. Louis, MO, USA). The proteins were transferred to polyvinylidene difluoride membranes and then reacted with anti-pSTAT3, anti-STAT3 (Cell Signaling Technology), or anti-actin antibodies (Santa Cruz Biotechnology, Santa Cruz, CA, USA). Horseradish peroxidase-goat anti-mouse or rabbit IgG (Invitrogen, Camarillo, CA, USA) was used as the secondary antibody. Immunoreactive bands were visualized using a Pierce Western Blotting Substrate Plus Kit (Thermo Scientific, Rockford, IL, USA) and ImageQuant LAS-4000 mini system (Fuji Film, Tokyo, Japan).

2.10. cDNA Microarray

OPCs and macrophages cultured in DMEM/F-12 supplemented with 10% FBS and penicillin/streptomycin for 2 days (pooled samples from three independent culture wells) were lysed using RNAiso Plus (Takara), and cDNA microarray analysis (SurePrint G3 Human Gene Expression

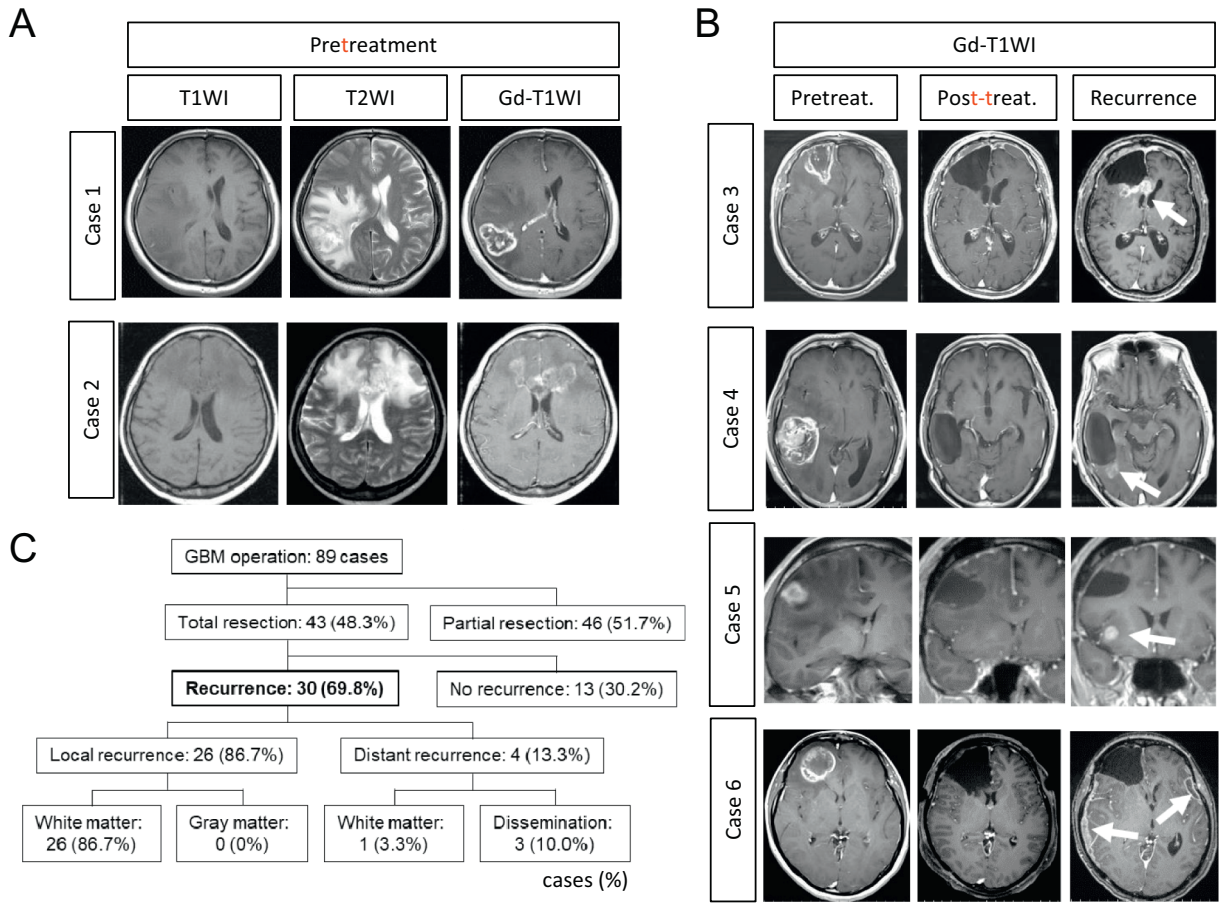

Fig. 1. GBM developed, invaded, and recurred in white matter. (A) GBM showing low- and high-intensity signals in T1- and T2-weighted MRI images. Irregular large high-intensity areas in T2-WIs showed vasogenic edema in the white matter accompanied by GBM cell invasion. Ring-like contrast-enhanced lesions in Gd-T1WIs showed the tumor mass lesion. Case 1: right parieto-temporal GBM. Case 2: bifrontal GBM connected corpus callosum, showing a butterfly shape. (B) Case 3: the enhanced mass lesion was removed completely; however, at 10 months after operation, GBM recurred in the corpus callosum and right frontal white matter. Case 4: 12 months after total resection, GBM recurred in the right occipital white matter. Case 5: 4 months after total resection, GBM recurred in the right insula white matter. Case 6: 2 months after total resection, GBM cells disseminated and formed enhanced mass lesions in the subaracnoid space. (C) In 89 patients with newly diagnosed GBM, complete resection was achieved in 43 cases (48.3%). Recurrence was observed in 30 cases (69.8%) in the complete resection group. Local recurrence was observed in 26 cases (86.7%), and distant recurrence was observed in four cases (13.3%). All local recurrence was observed in the white matter at the edge of the tumor removal cavity (26 cases; 86.7%). Three cases (10%) of subarachnoid dissemination were identified, but only one case (3.3%) showed distant recurrence in the white matter.

Microarray; Agilent Technologies) was performed with a Cell Inovator (Fukuoka, Japan). Expression data were deposited at NCBI Gene Expression Omnibus (GEO) under the accession number GSE 104742.

2.11. Statistics

To compare the three groups, one-way analysis of variance (ANOVA) was used, and data are presented as the mean ± SEM. All values from in vitro studies were representative results of two or three independent experiments. Data are expressed as the means ± standard deviation. Student's *t*-tests were used for comparisons of the two groups in our in vitro studies. $P < 0.05$ was considered statistically significant.

3. Results

3.1. GBM Recurrence Was Observed in the White Matter Attached to the Tumor Removal Cavity

Brain function, such as motor ability, sensory ability, and speech, is localized in specific areas, and such functional areas are also connected to the other important areas via bundles of nerve fibers. Generally, GBM develops in the white matter, and GBM cells start to spread along nerve fibers, such as association fibers and commissural fibers. The areas of perifocal edema around tumor mass showing low and high intensity in T1WI and T2WI in MRI are caused by increasing permeability to water due to invasion of GBM cells (Fig. 1A) (McMillan et al., 2009). Such perifocal edema is extended into the white matter. To avoid deterioration of brain function, neurosurgeons attempt to completely remove the main mass lesions detected with Gd-T1WI. However, despite complete removal of the lesion, we found that GBM commonly recurred within a year in the local white matter (Fig. 1B), but rarely in the distant area and subarachnoid space in the early stage of recurrence. To detect early recurrence and regrowth, MRI examination is typically performed every month for 2–3 years in our hospital.

In this study, we present data for 89 patients with newly diagnosed GBM admitted to our institution from January 2013 to December 2015; total resection was performed in 43 cases (48.3%), and partial resection was performed in 46 cases (51.7%). Total resection was defined as no residual enhanced tumor mass in Gd-T1WI and no other suspicious mass lesions in T2WIs. In the total resection group, no recurrence was observed in 13 cases (30.2%; mean duration of follow up: 19.1 months [3–36 months]), and recurrence was observed in 30 cases (69.8%) during the same study period. The site of recurrence first detected in Gd-T1WI was local in 26 cases (86.7%) and distant in four cases (13.3%; Fig. 1B–C). Local recurrence was characterized as tumor recurrence at the edge of the tumor removal cavity (cases 3 and 4), and distant recurrence was defined as tumor recurrence at a region separate from the removal cavity (case 5) and in the subarachnoid space (case 6). All local

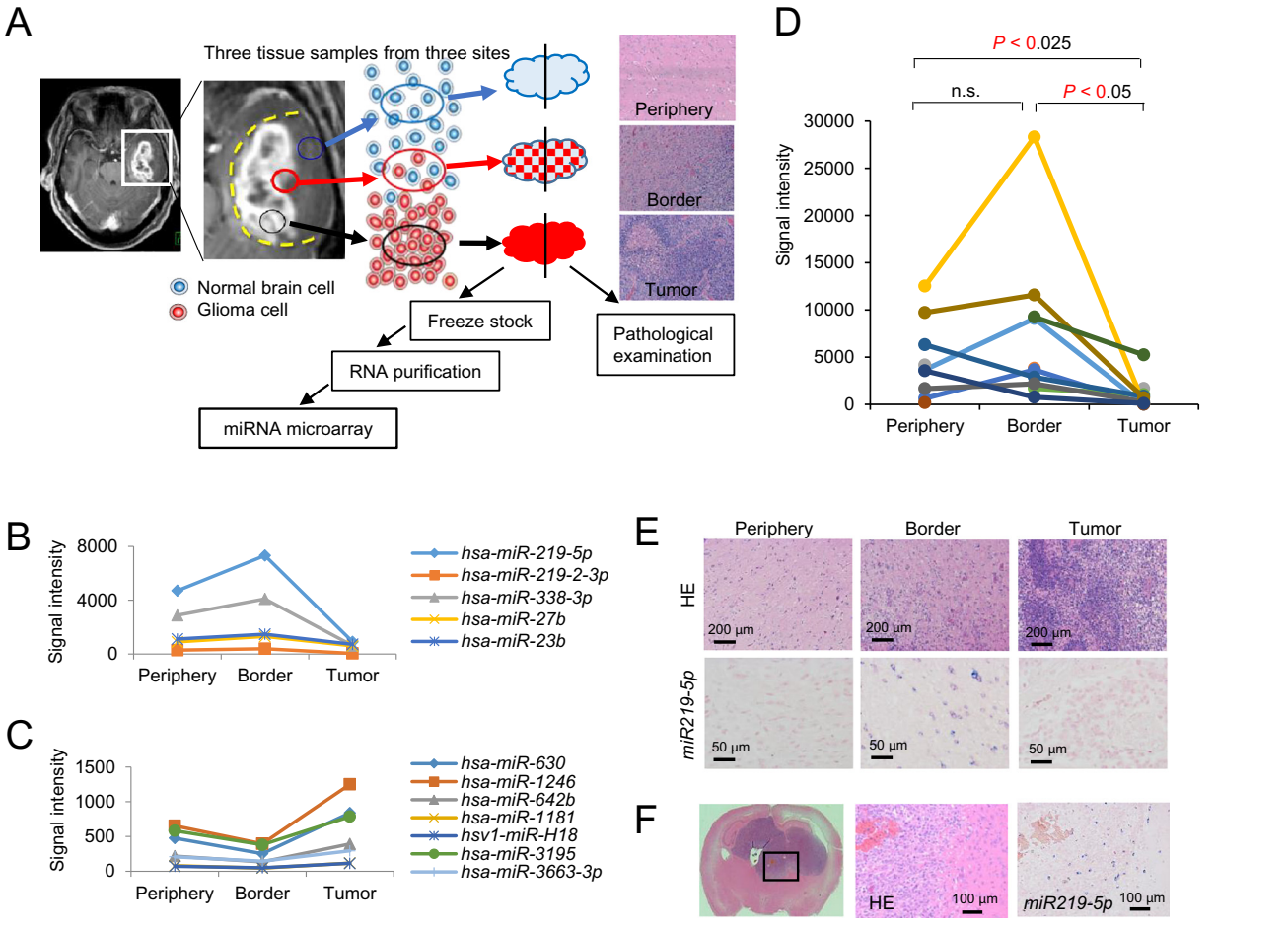

Fig. 2. Concept of this study and identified miRNAs. (A) GBMs usually recurred at the interface of white matter and tumor tissue. Three tissue samples were obtained from three regions (tumor, border, and periphery) and divided into two pieces. Half of the pieces were used for pathological examination. Pathologically, we defined the tumor as typical GBM tissue, the border as a mixture of tumor and normal cells, and the periphery as nearly normal brain tissue. We purified small RNAs from another piece after pathological confirmation and conducted miRNA microarray analysis. (B) Five miRNAs showed characteristically higher expression in the border. (C) Seven miRNAs showed characteristically lower expression in the border. (D) *miR-219-5p* showed significantly higher expression in the border and periphery compared with that in the tumor (periphery, $n = 9$: 4712 ± 1383; border, $n = 11$: 7323 ± 2608; tumor, $n = 10$: 1535 ± 463; mean ± standard errors of the mean [SEM], one-way analysis of variance [ANOVA]; n.s., nonsignificant). (E) In situ hybridization identified numbers of *miRNA-219-5p* positive cells in the border, but rare in the tumor. (F) *miRNA-219-5p* was detected in the border region of GSC xenografts from nude mouse brains.

recurrence was detected in white matter (86.7%), and not in gray matter (0%). Conversely, distant recurrence in white matter was identified in only one case (3.3%), but three other distant lesions were subarachnoid dissemination (10.0%; case 6) in the group showing recurrence (Fig. 1C and Table S1). Even after complete resection of the enhanced mass lesion, the majority of recurrent cases emerged in local white matter. These results and previous reports (Brandes et al., 2009) suggested that GBM cells in the border area, but not in the area distant from the enhanced tumor mass, survive after chemo-radiotherapy, resulting in local recurrence. Thus, a hotbed for recurrence of GBM exists in the white matter just around the tumor mass.

3.2. Identification of miRNAs Showing Characteristic Changes at the Interface between the Tumor and Brain

We hypothesized that studies of the white matter adjacent to the tumor mass could lead to the discovery of new mechanisms inducing chemo-radioresistance in GBM cells. To elucidate the features of the unique microenvironment required for GBM cells at the tumor border in white matter, we compared miRNA expression in samples from three sites in the resected tissue: the tumor mass (tumor), the border area between the tumor mass and brain where tumor and normal cells co-exist (border), and the peripheral area far from the tumor mass containing mostly normal cells (periphery), from individual patients (Fig. 2A). Abnormal tumor vessels were always identified in the tumor, but were rarely observed in the border (Fig. S1). In resected tissues, pathological features were confirmed by hematoxylin and eosin (HE) staining, and small RNAs were purified for miRNA microarray analysis (Fig. 2A and Fig. S1). Twenty sets of samples from GBM patients were examined (Table S2).

Upregulated miRNAs in the border region were defined as having more than two-fold higher expression than those in the tumor and periphery; downregulated miRNAs in the border region were defined as having less than half of the expression observed in the tumor and periphery. In results from 12 patients, five upregulated miRNAs (*miR-219-5p*, *miR-219-2-3p*, *miR-338-3p*, *miR-27b*, and *miR-23b*; Fig. 2B and Table S3) and seven downregulated miRNAs (*miR-630*, *miR-1246*, *miR-642b*, *miR-1181*, *miR-H18*, *miR-3195*, and *miR-3663-3p*) were identified (Fig. 2C and Table S4). The expression of *miR-219-5p* in the border and peripheral region was significantly higher than that in the tumor (Fig. 2D and Fig. S2A). When the data of the patient who showed the highest *miR-219-5p* expression were deleted, the expression of *miR-219-5p* in the border and peripheral region was still significantly higher (Fig. S2B). In our microarray data, lower expression of *miR-219-5p*, *miR-124*, and *miR-128* and higher expression of *miR-21* was observed in GBM compared with the peripheral region, similar to the results of previous reports (Fig. 2D and Fig. S3A) (Rao et al., 2013; Yang et al., 2015). Notably, *miR-219-5p* has been reported to function as a tumor suppressor in glioblastoma, hepatocellular carcinoma, papillary thyroid carcinoma, and colorectal cancer (Huang et al., 2015; Huang et al., 2012; Jiang et al., 2015; Rao et al., 2013; Xiong et al., 2015). In this study, we focused on *miR-219-5p* as a key molecule to reveal the special microenvironment of GBM cells allowing them to acquire chemo-radioresistance in the border region.

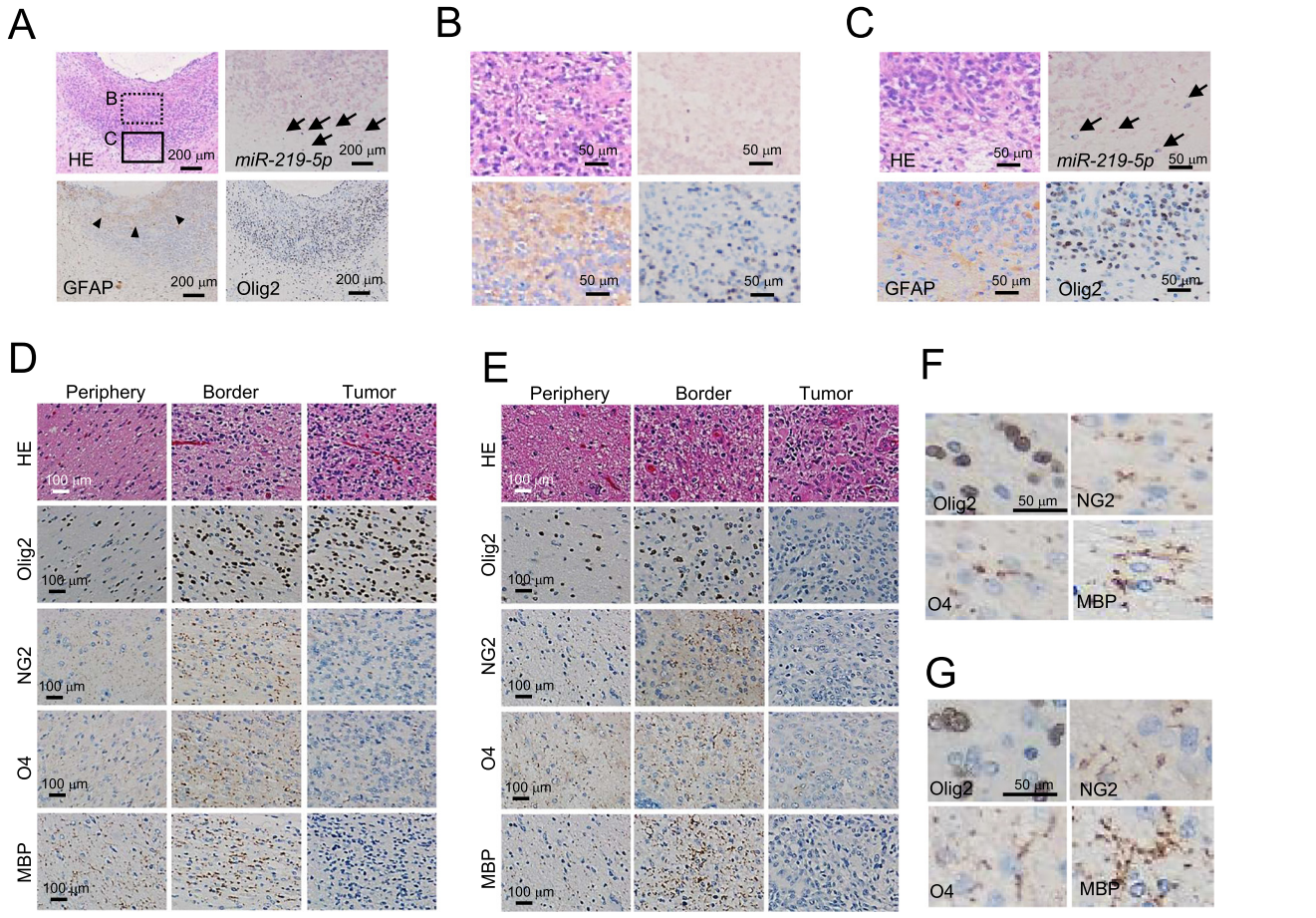

Fig. 3. Oligodendrocyte lineage cells were increased in the border, but not in the tumor. (A) Tumor tissues showed high cellularity on hematoxylin-eosin (HE) staining. GFAP-positive cells were strongly detected in the tumor; *miR-219-5p*-positive and Olig2-positive cells were observed in the border (B) Higher-magnification view in the tumor; GFAP positive cells were seen in the tumor but Olig2 positive cells were detected in outer areas. (C) Higher-magnification view in the periphery; *miR-219-5p*-positive and Olig2-positive cells were observed but GFAP = positive cells were rare. (D-G) A representative case from the $Olig2^{high}$ group (D and F) and the $Olig2^{low}$ group (E and G) in lower and higher magnification. Oligodendrocyte lineage markers, i.e., Olig2 and NG2 for OPCs, O4 for immature oligodendrocytes, and MBP for mature oligodendrocytes, were strongly detected in the border in both groups.

In situ hybridization was performed to confirm *miR-21* expression as a positive control in GBM (Fig. S3B), and increased numbers of *miR-219-5p*-positive cells were observed in the border region compared with the periphery, but not in the tumor (Fig. 2E). These results corresponded to our miRNA microarray data. Moreover, in mouse brains injected with GSCs established from resected GBM tissue of a 68 year-old male patient, the same distribution pattern of *miR-219-5p* was identified (Fig. 2F, Fig. S4A–B). Notably, *miR-219-5p*-positive cells were increased in the area in which tumor cells invaded into the white matter, but not in the clear interface between the tumor and brain (Fig. S4B).

3.3. Oligodendrocyte Lineage Cells (OLCs) were Increased in the Border

Interestingly, the top three miRNAs (*miR-219-5p*, *miR-219-2-3p*, and *miR-338-3p*) showing higher expression in the border region were related to oligodendrocyte differentiation (Barca-Mayo and Lu, 2012; Dugas et al., 2010; Zhao et al., 2010). Immunohistochemical staining of Olig2 for identification of oligodendrocyte progenitor cells (OPCs) and glial fibrillary acidic protein (GFAP) for identification of astrocytes was performed. The distribution pattern of Olig2^{+} cells was similar to that of *miR-219-5p* in the border, whereas GFAP^{+} cells were mainly found in the tumor (Fig. 3A–C).

Olig2 is expressed in not only OPCs in the normal brain but also GSCs in GBM (Kupp et al., 2016; Ligon et al., 2007; Lu et al., 2001; Marie et al., 2001; Suva et al., 2014; Wegener et al., 2015). Here, we analyzed 19 consecutive GBM samples that contained border tissues by HE staining. Olig2^{+} cells were characteristically observed in the border region in all GBMs, particularly where GBM cells began to invade into the white matter, but were not abundant at the clear interface between the tumor mass and normal brain. From the results of Olig2 staining, GBMs were classified into two groups (high and low) based on the rate of Olig2^{+} cells in the tumor. Olig2^{high} cases (n = 10, 52.6%) showed many positive cells in the tumor and border (Fig. 3D), whereas Olig2^{low} cases (n = 9, 47.4%) showed few positive cells in the tumor, but many cells in the border (Fig. 3E).

Cells positive for other oligodendrocyte lineage markers, such as O4, NG2 (also known as chondroitin sulfate proteoglycan 4), and myelin basic protein (MBP), were also consistently found in the border region of Olig2^{high} (Fig. 3D and F) and Olig2^{low} samples (Fig. 3E and G). These data suggest that most Olig2^{+} cells in the border region were OLCs.

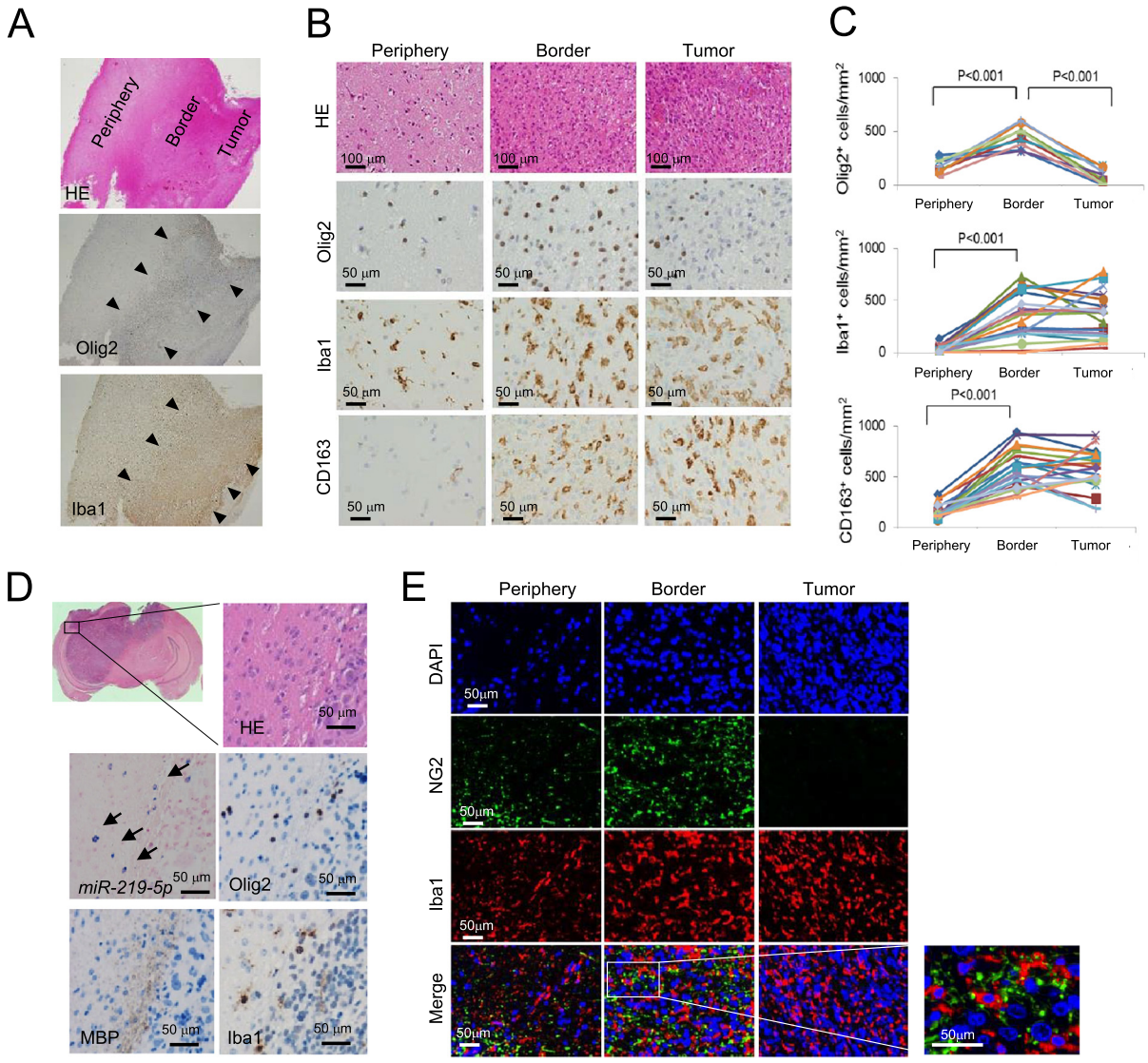

Fig. 4. OPCs increased in the border, and macrophages accumulated in the tumor and border. (A) In the Olig2^{low} group, Olig2^{+} cells were increased in the border but Iba1^{+} macrophages accumulated in the tumor and border in lower-magnification views. (B) In the Olig2^{low} group, Olig2^{+} cells were found in the border, and Iba1^{+} M1 macrophages and CD163^{+} M2 macrophages strongly accumulated in the tumor and border. (C) In the Olig2^{low} group, the number of Olig2^{+} cells was significantly increased in the border compared with that in the periphery ($p < 0.001$) and tumor ($p < 0.001$). Iba1- and CD163^{+} cells accumulated in the tumor and significantly in the border ($p < 0.001$). (D) *miR-219-5p*-, Olig2-, MBP-, and Iba1-positive cells were found in the border in a xenograft model. (E) In fluorescent immunohistochemical analysis, NG2-positive OPCs and Iba1-positive macrophages were colocalized in the border region.

3.4. Macrophages/Microglia Were Attracted to and Colocalized with OPCs in the Border

Infiltration of large numbers of macrophages/microglia into GBM tissues is commonly observed (Hambardzumyan et al., 2016; Komohara et al., 2012; Kuratsu et al., 1989; Pyonteck et al., 2013; Wei et al., 2013). Additionally, the anti-apoptotic function of *miR-219-5p* in macrophages has been reported (Lou et al., 2016). To confirm accumulation of macrophages in the border and tumor, immunohistochemical staining for Iba1 as a marker of tumor-suppressive macrophages/microglia and CD163 as a marker of tumor-promoting macrophages was performed. The numbers of $Iba1^+$ and $CD163^+$ macrophages were increased in both $Olig2^{high}$ and $Olig2^{low}$ samples. In $Olig2^{low}$ samples, the border region was readily detected by determination of the distribution of $Olig2^+$ cells (Fig. 4A). Both types of macrophages were significantly increased in the border and tumor regions compared with that in the periphery in nine $Olig2^{low}$ samples (Fig. 4B–C). Similar to human GBM samples, Olig2-, MBP-, and Iba1-positive cells were also increased in the border in the xenograft model (Fig. 4D). Moreover, $NG2^+$ OPCs were close to $Iba1^+$ macrophages/microglia in the border region of human GBM (Fig. 4E). These results indicated that OPCs and macrophages/microglia formed a characteristic environment in the border region.

3.5. Secreted Factors Derived from OPCs and Macrophages Increased Stemness Gene Expression in GBM Cells

To investigate whether OPCs, macrophages, and glioma cells interacted, we prepared conditioned medium (CM) from human OPCs (CM-OPC), human macrophages (CM-Mac), and human GBM cell lines (A172 [CM-A172] and T98G [CM-T98G]) and then cultured the cells in medium containing CM. OPC viability was significantly increased by CM-Mac, CM-A172, and CM-T98G (Fig. 5A). These results suggest that soluble factors derived from GBM increased the viability of OPCs. In migration assays, increased numbers of macrophages were attracted by CM-A172 and CM-T98G (Fig. 5B), similar to previous reports (Komohara et al., 2012; Kuratsu et al., 1989).

Next, we examined whether glioma cells acquired stem cell profiles by interaction with OPCs and macrophages. Real-time polymerase chain reaction (PCR) was used for quantification of the stemness-related genes *Nanog*, *Sox2*, aldehyde dehydrogenase isoform 1 (*ALDH1*), *Oct3/4*, and *Bmi1*. CM-OPC significantly upregulated the expression of *Sox2* and *Bmi1* in A172 cells and that of *Nanog*, *ALDH1*, *Oct3/4*, and *Bmi1* in T98G cells (Fig. 5C). CM-Mac induced significantly higher expression of *Sox2* and *Bmi1* in A172 cells and *Nanog*, *ALDH1*, *Oct3/4*, and *Bmi1* in T98G cells (Fig. 5D). These data demonstrate that both types of glioma cells acquired the expression of stemness genes and that different types of glioma cells showed varying sensitivity to OPCs and macrophages, but showed cell line-specific induction of stemness genes.

3.6. Glioma Cells Acquired Chemo-Radioresistant Properties through Interaction with OPCs and Macrophages

Next, to test whether GBM cells obtained stemness properties and treatment resistance by interacting with OPCs and macrophages, glioma cells were treated with CM from OPC/macrophage cocultures (CM-OM).

We performed sphere-forming and proliferation assays to determine how stem cell characteristics were acquired. To evaluate sphere forming ability, glioma cells were cultured in medium containing SphereMax (Wako, Tokyo, Japan) (Aihara et al., 2016) with CM in super low attachment plates. CM-OM significantly upregulated

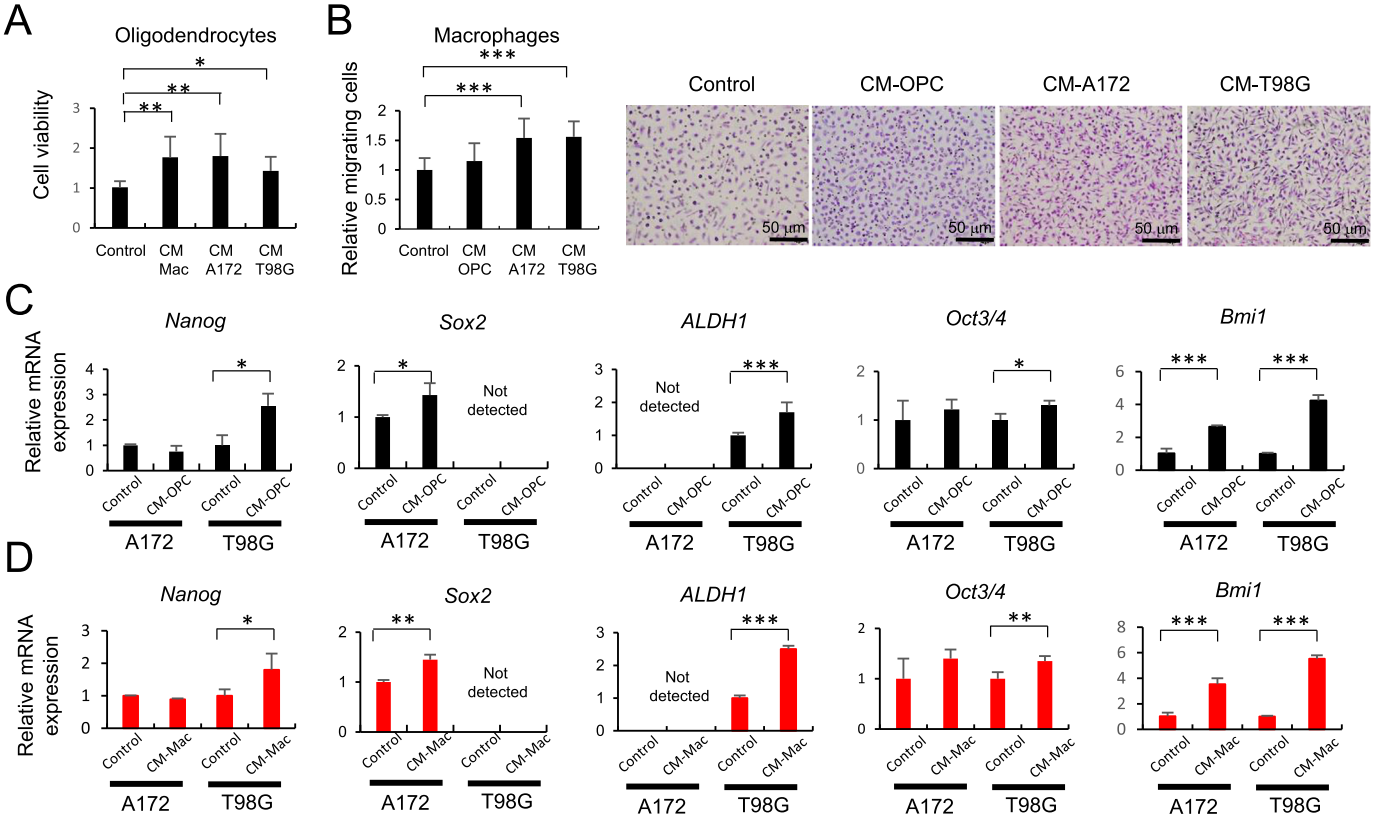

Fig. 5. GBM cells acquired stemness by interacting with OPCs and macrophages. (A) The relative viability of OPCs was increased significantly following treatment with conditioned medium plus CM-Mac ($p < 0.01$), CM-A172 ($p < 0.01$), and CM-T98G ($p < 0.05$) compared with that in the control. (B) The invasion ability of macrophages was increased by CM-OPC, CM-A172 ($p < 0.005$), and CM-T98G ($p < 0.005$). (C) CM-OPC increased the relative mRNA expression of *Sox2* ($p < 0.05$) and *Bmi1* ($p < 0.005$) in A172 and *Nanog* ($p < 0.05$), *ALDH1* ($p < 0.005$), *Oct3/4* ($p < 0.05$), and *Bmi1* ($p < 0.005$) in T98G. (D) CM-Mac increased the relative mRNA expression of *Sox2* ($p < 0.01$) and *Bmi1* ($p < 0.005$) in A172 and *Nanog* ($p < 0.05$), *ALDH1* ($p < 0.005$), *Oct3/4* ($p < 0.01$), and *Bmi1* ($p < 0.005$) in T98G.

sphere-forming ability and cell viability in both A172 and T98G cells (Fig. 6A–C). Additionally, the expression of ATP-binding cassette subfamily G member 2 (*ABCG2*), which is related to drug efflux ability, was significantly elevated in both A172 and T98G cells in real-time PCR (Fig. 6D). To confirm the acquisition of chemoresistance, we selected A172 cells, because A172 cells are TMZ sensitive, but T98G cells are resistant (Lee et al., 2011; Perazzoli et al., 2015). A172 cells cultured with CM were treated with TMZ, a standard therapeutic drug for GBM. Cell viability after treatment with TMZ was decreased by 70%, whereas addition of CM-OPC or CM-OM significantly recovered cell viability to 85% in A172 cells (Fig. 6E). Next, we analyzed the levels of phosphorylated signal transducer and activator of transcription 3 (pSTAT3) because pSTAT3 is important for radioresistance, immunosuppression, anti-apoptosis, stemness, and tumorigenesis (Jahani-Asl et al., 2016; Kaneko et al., 2015; Komohara et al., 2014). We found that the pSTAT3/STAT3 ratio was increased in A172 cells cultured with CM-OPC and CM-OM for 15 min (Fig. 6F). Thus, glioma cells affected by OPCs and macrophages exhibited significantly higher sphere-forming ability and chemoresistance and showed increased radioresistant potential. These data indicate that the chemo-radioresistance and recurrence of GBM could be attributed to the interactions with OPCs and macrophages.

3.7. FGF 1, EGF, HB-EGF, and IL-1β Increased Sphere-Forming Ability and Cell Viability in Glioma Cells

To identify soluble factors that promote stemness profiles in glioma cells, DNA microarray analysis was performed. A172 and T98G possessed different sensitivities to CM-OPC and CM-Mac, indicating that CM-OPC and CM-Mac contained different characteristic soluble factors. From the microarray data, we selected some candidate genes that showed higher and differential expression patterns between OPCs and macrophages (Fig. 7A). Here, A172 cells, which were more sensitive to CM-OPC, were cultured with candidate factors (10 ng/mL) showing higher expression in OPCs, such as insulin-like growth factor-2 (IGF-2), IGF-binding protein 3 (IGF-BP3), FGF-1, vascular endothelial growth factor-C (VEGF-C), placental growth factor-1 (PIGF-1), EGF-containing fiburin-like extracellular matrix protein 1 (EFEMP1), and EGF. The viability of A172 cells was increased by culturing with all the selected factors as compared with the control; in particular, the number of spheres and viability of cells after culture with FGF1 and EGF were increased more than that of cells cultured with CM-OPC (Fig. 7B–C). T98G cells, which were more sensitive to CM-Mac, were cultured with candidate factors (10 ng/mL) showing higher expression in macrophages, such as osteopontin (OPN), HB-EGF, oncostatin M (OSM), IL-6, I309, tumor necrosis factor (TNF), IL-1β, and C5a. HB-EGF and IL-1β increased sphere-forming ability and cell viability similarly to CM-Mac (Fig. 7D–E). These data suggest that GBM cells in the border colocalize with OPCs and macrophages/microglia, and that growth factors and cytokines secreted from these cells promote stemness profiles and chemo-radioresistance in GBM cells. These crosstalk events, which include OPCs, macrophages/microglia, and GBM cells, in the border may be promising targets for preventing recurrence and prolonging survival in patients with GBM (Fig. 7F).

4. Discussion

Clinically, GBM develops, invades, and recurs in white matter, where abundant OPCs proliferate and differentiate into myelinating mature oligodendrocytes. OPCs represent the majority of proliferating cells in the adult brain and exhibit specific characteristics; for example, individual OPCs occupy their own territory, and OPC density is maintained through local proliferation. Additionally, OPCs migrate rapidly to the injured site (Hughes et al., 2013) and occupy regions of traumatic brain injury

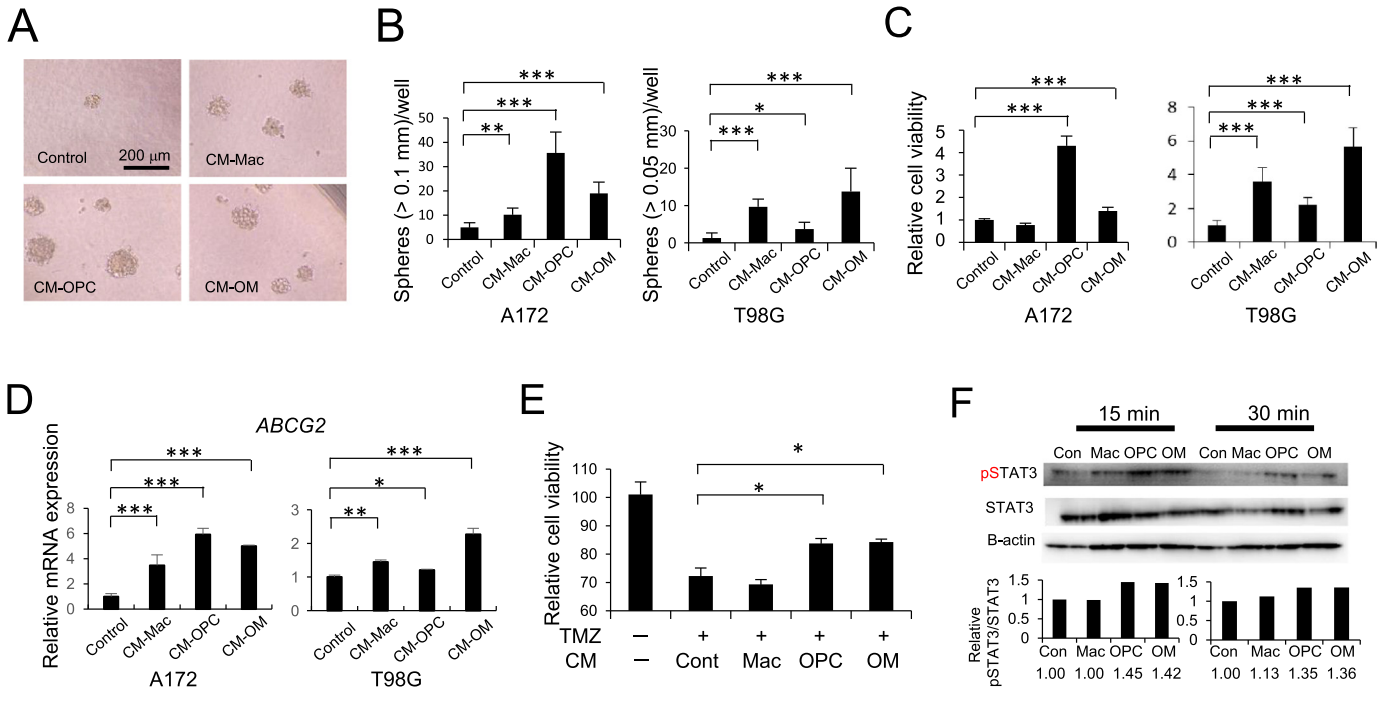

Fig. 6. Conditioned medium derived from OPCs and macrophages induced stemness and chemo-radioresistant abilities. (A) Photographs of T98G spheres cultured in medium with the control (without CM), CM-Mac, CM-OPC, and CM-MO. (B) Sphere-forming ability in A172 cells cultured with CM-Mac ($p < 0.01$), CM-OPC ($p < 0.005$), and CM-MO ($p < 0.005$) increased relative to that in the control. Sphere-forming ability in T98G cells cultured with CM-Mac ($p < 0.005$), CM-OPC ($p < 0.05$), and CM-MO ($p < 0.005$) also increased relative to that in the control. (C) Viability in A172 cells cultured with CM-Mac, CM-OPC ($p < 0.005$), and CM-MO ($p < 0.005$) increased significantly, and that in T98G cells cultured with CM-Mac ($p < 0.005$), CM-OPC ($p < 0.005$), and CM-MO ($p < 0.005$) increased significantly relative to that of the control. (D) Relative mRNA expression of *ABCG2* was increased by CM-Mac ($p < 0.005$), CM-OPC ($p < 0.005$), and CM-MO ($p < 0.005$) in A172 cells and was also increased by CM-Mac ($p < 0.01$), CM-OPC ($p < 0.05$), and CM-MO ($p < 0.005$) in T98G cells. (E) Resistance to the chemotherapeutic agent temozolomide (TMZ) in A172 cells was induced by CM-OPC ($p < 0.05$) and CM-MO ($p < 0.05$). (F) In western blot analysis, the relative p-STAT3/STAT3 ratio was increased by CM-OPC and CM-MO in 15 min; the increase was maintained by treatment with CM-OPC and CM-MO for 30 min.

within 1 day (Dimou and Gallo, 2015), which is faster than the reaction of astrocytes (Fernandez-Castaneda and Gaultier, 2016). Neuronal activity also remodels white matter rapidly, and running stimulates OPC proliferation and oligodendrocyte production within only a few days (McKenzie et al., 2014). Additionally, OPCs may be cell of origin for GBM (Galvao et al., 2014; Hide et al., 2011; Liu et al., 2011; Sugiarto et al., 2011). Thus, based on proliferation potential, OPCs have been discussed with regard to gliomagenesis, but not with regard to their supportive function for GBM cells.

In this study, all local recurrent lesions appeared in white matter, and not in gray matter. Young et al. reported that OPCs in forebrain white matter (corpus callosum) have a shorter cell division cycle (~10 days) than those in gray matter (motor cortex; ~36 days) of the mouse brain at 60 days after birth (Young et al., 2013). Moreover, from single-cell RNA sequencing in 5072 cells, OLCs were classified into 13 populations showing region- and age-specific distributions (Marques et al., 2016). Further studies are needed to determine functional variations in OLCs in the development and recurrence of GBM.

Macrophages/microglia have contradictory roles in promoting and preventing GBM growth. Pyonteck et al. reported that co-injection of macrophages with glioma cells enhanced tumor growth by 62% compared with injection of glioma cells alone. Moreover, macrophages and glioma cells have reciprocal effects on survival, proliferation, and/or polarization of each other to promote tumorigenesis (Pyonteck et al., 2013). One important tumor-promoting mechanism is that glioma cells decrease basal caspase-3 activity in microglia, thereby supporting glioma tumor growth (Shen et al., 2016). Conversely, Sarkar reported that activation of macrophages and microglia by amphotericin B (Amp B) suppresses the sphere-forming ability of GSCs and that Amp B treatment reduces tumor growth and prolongs survival of mice with

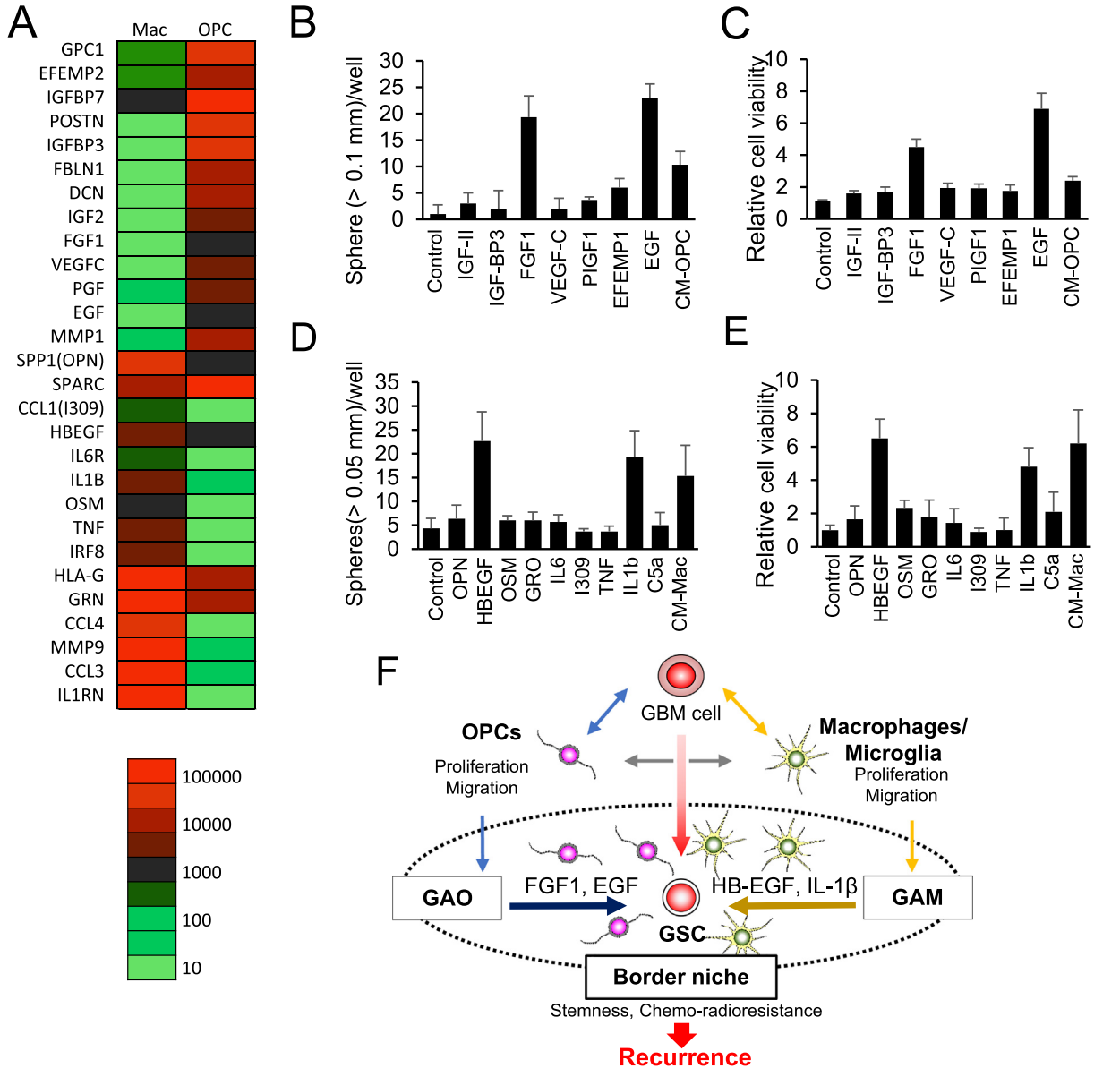

Fig. 7. FGF1 and EGF from OPCs and HB-EGF and IL-1β from macrophages reproduced the sphere forming ability and cell viability observed in GBM cells. (A) Heat map showing the representative genes expressed in OPCs and macrophages. (B, C) Sphere-forming ability (>100 μm/well) and cell viability following addition of selected growth factors and cytokines (10 ng/mL) in A172 cells. (D, E) Sphere-forming ability (>50 μm/well) and cell viability following addition of selected growth factors and cytokines (10 ng/mL) in T98G cells. (F) Scheme showing the concept of a "border niche". GBM cells affected OPCs and macrophages, and macrophages interacted with OPCs. Accumulated OPCs secreted FGF1 and EGF, and macrophages produced HB-EGF and IL-1β, conferring stemness and chemo-radioresistant potential on GBM cells, similar to GSCs. Interactions of OPCs, macrophages, and GBM cells resulted in formation of the border niche, in which OPCs functioned as glioma-associated oligodendrocytes (GAOs) and macrophages functioned as glioma-associated macrophages/microglia (GAMs). GBM cells in the border niche caused recurrence.

xenograft tumors (Sarkar et al., 2014). Furthermore, inhibition of colony-stimulating factor-1 receptor reprograms macrophages to become antitumorigenic (Quail et al., 2016). Based on these studies, recruited macrophages and microglia have fundamental roles in the progression of glioma. Glioblastoma-associated microglia and macrophages are thought to function as therapeutic targets inhibiting immunosuppression, invasion, and angiogenesis (Poon et al., 2017), and our data suggest that macrophages/microglia induce stemness and chemoradioresistance in GBM cells.

Astrocytes were not evaluated in this study because GFAP-positive cells were detected in the tumor, border, and peripheral region. However, astrocytes seemed to play indirect roles in the formation of the GSC niche at the border because astrocytes affect the proliferation and remyelination of OPCs (Lundgaard et al., 2014; Moore et al., 2011). Additionally, brain-derived neurotrophic factor (BDNF) secreted by astrocytes promotes oligodendrogenesis after white matter damage (Miyamoto et al., 2015). In contrast, astrocytes have a low proliferation rate and migration potential to sites of wound injury (Bardehle et al., 2013). OPCs and microglia, but not astrocytes, play an immediate role in central nervous system injury (Fernandez-Castaneda and Gaultier, 2016). Thus, the rapid reaction potential of OPCs and macrophages/microglia provides advantages for GBM cells in the formation of the GSC niche in the border because GBM cells possess higher proliferation and migration potential, thereby necessitating rapid adaptation of supportive cells.

Several growth factors and cytokines are related to tumor growth. C-C motif chemokine ligand 2 (CCL-2), also known as monocyte chemoattractant protein 1 (MCP-1), is a major chemokine that acts as a glioma cell-derived monocyte chemotactic factor (Kuratsu et al., 1989). Moyan reported that CCL-2 and IL-1β levels are increased in activated OPCs and within areas of cuprizone-induced demyelination in the mouse brain. Overexpression of CCL-2 in OPCs results in increased migration (Moyon et al., 2015). Conversely, stromal cells such as macrophages secrete more CCL-2 into the cancer microenvironment than cancer cells (Salacz et al., 2016; Yoshimura, 2017). In a positive feedback loop, GBM cells secrete CCL-2 and attract OPCs and macrophages/microglia; these cells also secrete CCL-2, and the number of activated cells is increased, resulting in the development of the GSC niche. Indeed, in our analysis, CCL-2 expression was higher in both OPCs and macrophages. Thus, GBM cells, OPCs, and macrophages/microglia exhibited a robust reciprocal network in proliferation, migration, and stemness.

GSCs are commonly cultured in medium containing FGF2 and EGF, but not FGF1. Expression of FGF1 and EGF in OPCs increased the numbers of spheres and viability of A172 cells. FGF1 is the most abundant FGF in white matter and suppresses the differentiation of OPCs (Mohan et al., 2014). Additionally, activation of Aurora A kinase through the FGF1/FGFR signaling axis sustains the stem cell characteristics of GBM cells (Hsu et al., 2016). Thus, FGF1 in the white matter is essential for acquisition and maintenance of stemness. Moreover, expression of HB-EGF and IL-1β in macrophages significantly increased sphere-forming ability and viability in T98G cells. HB-EGF is a member of the EGF family, and has been reported to activate mitogenic signaling and to show increased expression in human malignant gliomas (Mishima et al., 1998). In contrast, IL-1β is expressed rapidly in response to neuronal injury, predominantly by microglia, and is associated with the pro-inflammatory response (Simi et al., 2007). IL-1β promotes tumor growth and increases the cancer stem cell phenotype in glioma cells by activating the p38 mitogen-activated protein kinase signaling pathway and inducing expression of MCP-1 (Feng et al., 2015). Taken together, our findings demonstrate that these factors are closely associated with GBM cells, OPCs, and macrophage/microglia and induce stem cell profiles in GBM cells. Thus, our data and previous reports suggest that during tumor growth, OPCs and macrophages/microglia migrate and proliferate rapidly in the border region, where they secrete growth factors and cytokines, causing GBM cells to acquire stem cell profiles and chemo-radioresistance. Accordingly, we propose that this sanctuary for GBM cells in the border be called the “border niche”, in which OPCs and macrophages/microglia function as glioma-associated oligodendrocytes (GAOs) and glioma-associated macrophages/microglia (GAMs), respectively, similar to cancer-associated fibroblasts and tumor-associated macrophages in other cancers (Fig. 7G).

In summary, our data provide important insights into the essential features of the border niche for chemo-radioresistance and recurrence, representing a promising treatment target. In particular, GAOs may be critical target cells that should be studied in greater detail. Moreover, further studies of the border niche are needed to improve clinical outcomes and prevent recurrence in patients with GBM.

Supplementary data to this article can be found online at https://doi.org/10.1016/j.ebiom.2018.02.024.

Acknowledgements

We would like to thank Masayo Obata for technical assistance.

Funding Sources

This work was supported by a Grant-in-Aid for Scientific Research on Innovative Areas “Development of Novel Treatment Strategies Targeting Cancer Stem Cells” (to T. Hide; nos.: 23130512 and 25130710).

Conflicts of Interest

There are no conflicts of interest.

Author Contributions

T. H. conceived this study. T. H., Y. K., and Y. M. performed in vivo and in vitro experiments. H. N., K. M., and J. K. acquired patient specimens and clinical data. A. M. supported interpretation of clinical data. M. T., J. K. and S. Y. supervised the study and edited the manuscript. T. H. and Y. K. analyzed and interpreted data and wrote the manuscript.

References

Aihara, A., Abe, N., Saruhashi, K., Kanaki, T., Nishino, T., 2016. Novel 3-D cell culture system for in vitro evaluation of anticancer drugs under anchorage-independent conditions. Cancer Sci. 107, 1858–1866.

Anai, S., Hide, T., Takezaki, T., Kuroda, J., Shinojima, N., Makino, K., Nakamura, H., Yano, S., Kuratsu, J., 2014. Antitumor effect of fibrin glue containing temozolomide against malignant glioma. Cancer Sci. 105, 583–591.

Barca-Mayo, O., Lu, Q.R., 2012. Fine-tuning oligodendrocyte development by microRNAs. Front. Neurosci. 6, 13.

Bardehle, S., Kruger, M., Buggenthin, F., Schwausch, J., Ninkovic, J., Clevers, H., Snippert, H.J., Theis, F.J., Meyer-Luehmann, M., Bechmann, I., et al., 2013. Live imaging of astrocyte responses to acute injury reveals selective juxtavascular proliferation. Nat. Neurosci. 16, 580–586.

Brandes, A.A., Tosoni, A., Franceschi, E., Sotti, G., Frezza, G., Amista, P., Morandi, L., Spagnolli, F., Ermani, M., 2009. Recurrence pattern after temozolomide concomitant with and adjuvant to radiotherapy in newly diagnosed patients with glioblastoma: correlation with MGMT promoter methylation status. J. Clin. Oncol. 27, 1275–1279.

Charles, N.A., Holland, E.C., Gilbertson, R., Glass, R., Kettenmann, H., 2011. The brain tumor microenvironment. Glia 59, 1169–1180.

Dimou, L., Gallo, V., 2015. NG2-glia and their functions in the central nervous system. Glia 63, 1429–1451.

Dugas, J.C., Cuellar, T.L., Scholze, A., Ason, B., Ibrahim, A., Emery, B., Zamanian, J.L., Foo, L.C., McManus, M.T., Barres, B.A., 2010. Dicer1 and miR-219 are required for normal oligodendrocyte differentiation and myelination. Neuron 65, 597–611.

Feng, X., Szulzewsky, F., Yerevanian, A., Chen, Z., Heinzmann, D., Rasmussen, R.D., Alvarez-Garcia, V., Kim, Y., Wang, B., Tamagno, I., et al., 2015. Loss of CX3CR1 increases accumulation of inflammatory monocytes and promotes gliomagenesis. Oncotarget 6, 15077–15094.

Fernandez-Castaneda, A., Gaultier, A., 2016. Adult oligodendrocyte progenitor cells - multifaceted regulators of the CNS in health and disease. Brain Behav. Immun. 57, 1–7.

Fidoamore, A., Cristiano, L., Antonosante, A., d'Angelo, M., Di Giacomo, E., Astarita, C., Giordano, A., Ippoliti, R., Benedetti, E., Cimini, A., 2016. Glioblastoma stem cells microenvironment: the paracrine roles of the niche in drug and radioresistance. Stem Cells Int. 2016, 6809105.

Galvao, R.P., Kasina, A., McNeill, R.S., Harbin, J.E., Foreman, O., Verhaak, R.G., Nishiyama, A., Miller, C.R., Zong, H., 2014. Transformation of quiescent adult oligodendrocyte precursor cells into malignant glioma through a multistep reactivation process. Proc. Natl. Acad. Sci. U. S. A. 111, E4214–4223.

Hambardzumyan, D., Gutmann, D.H., Kettenmann, H., 2016. The role of microglia and macrophages in glioma maintenance and progression. Nat. Neurosci. 19, 20–27.
Hide, T., Takezaki, T., Nakatani, Y., Nakamura, H., Kuratsu, J., Kondo, T., 2011. Combination of a ptgs2 inhibitor and an epidermal growth factor receptor-signaling inhibitor prevents tumorigenesis of oligodendrocyte lineage-derived glioma-initiating cells. Stem Cells 29, 590–599.
Hide, T., Makino, K., Nakamura, H., Yano, S., Anai, S., Takezaki, T., Kuroda, J., Shinojima, N., Ueda, Y., Kuratsu, J., 2013. New treatment strategies to eradicate cancer stem cells and niches in glioblastoma. Neurol. Med. Chir. (Tokyo) 53, 764–772.
Hsu, Y.C., Kao, C.Y., Chung, Y.F., Lee, D.C., Liu, J.W., Chiu, I.M., 2016. Activation of Aurora A kinase through the FGF1/FGFR signaling axis sustains the stem cell characteristics of glioblastoma cells. Exp. Cell Res. 344, 153–166.
Huang, N., Lin, J., Ruan, J., Su, N., Qing, R., Liu, F., He, B., Lv, C., Zheng, D., Luo, R., 2012. MiR-219-5p inhibits hepatocellular carcinoma cell proliferation by targeting glypican-3. FEBS Lett. 586, 884–891.
Huang, C., Cai, Z., Huang, M., Mao, C., Zhang, Q., Lin, Y., Zhang, X., Tang, B., Chen, Y., Wang, X., et al., 2015. miR-219-5p modulates cell growth of papillary thyroid carcinoma by targeting estrogen receptor alpha. J. Clin. Endocrinol. Metab. 100, E204–213.
Hughes, E.G., Kang, S.H., Fukaya, M., Bergles, D.E., 2013. Oligodendrocyte progenitors balance growth with self-repulsion to achieve homeostasis in the adult brain. Nat. Neurosci. 16, 668–676.
Ishii, A., Kimura, T., Sadahiro, H., Kawano, H., Takubo, K., Suzuki, M., Ikeda, E., 2016. Histological characterization of the tumorigenic "peri-necrotic niche" harboring quiescent stem-like tumor cells in glioblastoma. PLoS One 11, e0147366.
Jahani-Asl, A., Yin, H., Soleimani, V.D., Haque, T., Luchman, H.A., Chang, N.C., Sincennes, M.C., Puram, S.V., Scott, A.M., Lorimer, I.A., et al., 2016. Control of glioblastoma tumorigenesis by feed-forward cytokine signaling. Nat. Neurosci. 19, 798–806.
Jiang, Y., Yin, L., Jing, H., Zhang, H., 2015. MicroRNA-219-5p exerts tumor suppressor function by targeting ROBO1 in glioblastoma. Tumour Biol. 36, 8943–8951.
Kaneko, S., Nakatani, Y., Takezaki, T., Hide, T., Yamashita, D., Ohtsu, N., Ohnishi, T., Terasaka, S., Houkin, K., Kondo, T., 2015. Ceacam1L modulates STAT3 signaling to control the proliferation of glioblastoma-initiating cells. Cancer Res. 75, 4224–4234.
Kohlhapp, F.J., Mitra, A.K., Lengyel, E., Peter, M.E., 2015. MicroRNAs as mediators and communicators between cancer cells and the tumor microenvironment. Oncogene 34 (48), 5857–5868.
Komohara, Y., Horlad, H., Ohnishi, K., Fujiwara, Y., Bai, B., Nakagawa, T., Suzu, S., Nakamura, H., Kuratsu, J., Takeya, M., 2012. Importance of direct macrophage-tumor cell interaction on progression of human glioma. Cancer Sci. 103, 2165–2172.
Komohara, Y., Jinushi, M., Takeya, M., 2014. Clinical significance of macrophage heterogeneity in human malignant tumors. Cancer Sci. 105, 1–8.
Kros, J.M., Mustafa, D.M., Dekker, L.J., Sillevis Smitt, P.A., Luider, T.M., Zheng, P.P., 2015. Circulating glioma biomarkers. Neuro-Oncology 17, 343–360.
Kupp, R., Shtayer, L., Tien, A.C., Szeto, E., Sanai, N., Rowitch, D.H., Mehta, S., 2016. Lineage-restricted OLIG2-RTK signaling governs the molecular subtype of glioma stem-like cells. Cell Rep. 16, 2838–2845.
Kuratsu, J., Leonard, E.J., Yoshimura, T., 1989. Production and characterization of human glioma cell-derived monocyte chemotactic factor. J. Natl. Cancer Inst. 81, 347–351.
Lee, E.S., Ko, K.K., Joe, Y.A., Kang, S.G., Hong, Y.K., 2011. Inhibition of STAT3 reverses drug resistance acquired in temozolomide-resistant human glioma cells. Oncol. Lett. 2, 115–121.
Li, C., Sun, J., Xiang, Q., Liang, Y., Zhao, N., Zhang, Z., Liu, Q., Cui, Y., 2016. Prognostic role of microRNA-21 expression in gliomas: a meta-analysis. J. Neuro-Oncol. 130 (1), 11–17.
Ligon, K.L., Huillard, E., Mehta, S., Kesari, S., Liu, H., Alberta, J.A., Bachoo, R.M., Kane, M., Louis, D.N., Depinho, R.A., et al., 2007. Olig2-regulated lineage-restricted pathway controls replication competence in neural stem cells and malignant glioma. Neuron 53, 503–517.
Liu, C., Sage, J.C., Miller, M.R., Verhaak, R.G., Hippenmeyer, S., Vogel, H., Foreman, O., Bronson, R.T., Nishiyama, A., Luo, L., et al., 2011. Mosaic analysis with double markers reveals tumor cell of origin in glioma. Cell 146, 209–221.
Liu, X., Madhankumar, A.B., Miller, P.A., Duck, K.A., Hafenstein, S., Rizk, E., Slagle-Webb, B., Sheehan, J.M., Connor, J.R., Yang, Q.X., 2016. MRI contrast agent for targeting glioma: interleukin-13 labeled liposome encapsulating gadolinium-DTPA. Neuro-Oncology 18, 691–699.
Lou, W., Zhang, X., Hu, X.Y., Hu, A.R., 2016. MicroRNA-219-5p inhibits morphine-induced apoptosis by targeting key cell cycle regulator WEE1. Med. Sci. Monit. 22, 1872–1879.
Lu, Q.R., Park, J.K., Noll, E., Chan, J.A., Alberta, J., Yuk, D., Alzamora, M.G., Louis, D.N., Stiles, C.D., Rowitch, D.H., et al., 2001. Oligodendrocyte lineage genes (OLIG) as molecular markers for human glial brain tumors. Proc. Natl. Acad. Sci. U. S. A. 98, 10851–10856.
Lundgaard, I., Osorio, M.J., Kress, B.T., Sanggaard, S., Nedergaard, M., 2014. White matter astrocytes in health and disease. Neuroscience 276, 161–173.
Marie, Y., Sanson, M., Mokhtari, K., Leuraud, P., Kujas, M., Delattre, J.Y., Poirier, J., Zalc, B., Hoang-Xuan, K., 2001. OLIG2 as a specific marker of oligodendroglial tumour cells. Lancet 358, 298–300.
Marques, S., Zeisel, A., Codeluppi, S., van Bruggen, D., Mendanha Falcao, A., Xiao, L., Li, H., Haring, M., Hochgerner, H., Romanov, R.A., et al., 2016. Oligodendrocyte heterogeneity in the mouse juvenile and adult central nervous system. Science 352, 1326–1329.
McKenzie, I.A., Ohayon, D., Li, H., de Faria, J.P., Emery, B., Tohyama, K., Richardson, W.D., 2014. Motor skill learning requires active central myelination. Science 346, 318–322.
McMillan, K.M., Ehtesham, M., Stevenson, C.B., Edgeworth, M.L., Thompson, R.C., Price, R.R., 2009. T2 detection of tumor invasion within segmented components of glioblastoma multiforme. J. Magn. Reson. Imaging 29, 251–257.
Mishima, K., Higashiyama, S., Asai, A., Yamaoka, K., Nagashima, Y., Taniguchi, N., Kitanaka, C., Kirino, T., Kuchino, Y., 1998. Heparin-binding epidermal growth factor-like growth factor stimulates mitogenic signaling and is highly expressed in human malignant gliomas. Acta Neuropathol. 96, 322–328.
Miyamoto, N., Maki, T., Shindo, A., Liang, A.C., Maeda, M., Egawa, N., Itoh, K., Lo, E.K., Lok, J., Ihara, M., et al., 2015. Astrocytes promote oligodendrogenesis after white matter damage via brain-derived neurotrophic factor. J. Neurosci. 35, 14002–14008.
Mohan, H., Friese, A., Albrecht, S., Krumbholz, M., Elliott, C.L., Arthur, A., Menon, R., Farina, C., Junker, A., Stadelmann, C., et al., 2014. Transcript profiling of different types of multiple sclerosis lesions yields FGF1 as a promoter of remyelination. Acta Neuropathol. Commun. 2, 168.
Moore, C.S., Abdullah, S.L., Brown, A., Arulpragasam, A., Crocker, S.J., 2011. How factors secreted from astrocytes impact myelin repair. J. Neurosci. Res. 89, 13–21.
Moyon, S., Dubessy, A.L., Aigrot, M.S., Trotter, M., Huang, J.K., Dauphinot, L., Potier, M.C., Kerninon, C., Melik Parsadaniantz, S., Franklin, R.J., et al., 2015. Demyelination causes adult CNS progenitors to revert to an immature state and express immune cues that support their migration. J. Neurosci. 35, 4–20.
Perazzoli, G., Prados, J., Ortiz, R., Caba, O., Cabeza, L., Berdasco, M., Gonzalez, B., Melguizo, C., 2015. Temozolomide resistance in glioblastoma cell lines: implication of MGMT, MMR, P-glycoprotein and CD133 expression. PLoS One 10, e0140131.
Poon, C.C., Sarkar, S., Yong, V.W., Kelly, J.J.P., 2017. Glioblastoma-associated microglia and macrophages: targets for therapies to improve prognosis. Brain 140, 1548–1560.
Pyonteck, S.M., Akkari, L., Schuhmacher, A.J., Bowman, R.L., Sevenich, L., Quail, D.F., Olson, O.C., Quick, M.L., Huse, J.T., Teijeiro, V., et al., 2013. CSF-1R inhibition alters macrophage polarization and blocks glioma progression. Nat. Med. 19, 1264–1272.
Quail, D.F., Joyce, J.A., 2017. The microenvironmental landscape of brain tumors. Cancer Cell 31, 326–341.
Quail, D.F., Bowman, R.L., Akkari, L., Quick, M.L., Schuhmacher, A.J., Huse, J.T., Holland, E.C., Sutton, J.C., Joyce, J.A., 2016. The tumor microenvironment underlies acquired resistance to CSF-1R inhibition in gliomas. Science 352, aad3018.
Rao, S.A., Arimappamagan, A., Pandey, P., Santosh, V., Hegde, A.S., Chandramouli, B.A., Somasundaram, K., 2013. miR-219-5p inhibits receptor tyrosine kinase pathway by targeting EGFR in glioblastoma. PLoS One 8, e63164.
Salacz, M.E., Kast, R.E., Saki, N., Bruning, A., Karpel-Massler, G., Halatsch, M.E., 2016. Toward a noncytotoxic glioblastoma therapy: blocking MCP-1 with the MTZ regimen. Oncol. Targets Ther. 9, 2535–2545.
Sarkar, S., Doring, A., Zemp, F.J., Silva, C., Lun, X., Wang, X., Kelly, J., Hader, W., Hamilton, M., Mercier, P., et al., 2014. Therapeutic activation of macrophages and microglia to suppress brain tumor-initiating cells. Nat. Neurosci. 17, 46–55.
Shen, X., Burguillos, M.A., Osman, A.M., Frijhoff, J., Carrillo-Jimenez, A., Kanatani, S., Augsten, M., Saidi, D., Rodhe, J., Kavanagh, E., et al., 2016. Glioma-induced inhibition of caspase-3 in microglia promotes a tumor-supportive phenotype. Nat. Immunol. 17, 1282–1290.
Simi, A., Tsakiri, N., Wang, P., Rothwell, N.J., 2007. Interleukin-1 and inflammatory neurodegeneration. Biochem. Soc. Trans. 35, 1122–1126.
Singh, S.K., Hawkins, C., Clarke, I.D., Squire, J.A., Bayani, J., Hide, T., Henkelman, R.M., Cusimano, M.D., Dirks, P.B., 2004. Identification of human brain tumour initiating cells. Nature 432, 396–401.
Stupp, R., Hegi, M.E., Mason, W.P., van den Bent, M.J., Taphoorn, M.J., Janzer, R.C., Ludwin, S.K., Allgeier, A., Fisher, B., Belanger, K., et al., 2009. Effects of radiotherapy with concomitant and adjuvant temozolomide versus radiotherapy alone on survival in glioblastoma in a randomised phase III study: 5-year analysis of the EORTC-NCIC trial. Lancet Oncol. 10, 459–466.
Sturm, D., Witt, H., Hovestadt, V., Khuong-Quang, D.A., Jones, D.T., Konermann, C., Pfaff, E., Tonjes, M., Sill, M., Bender, S., et al., 2012. Hotspot mutations in H3F3A and IDH1 define distinct epigenetic and biological subgroups of glioblastoma. Cancer Cell 22, 425–437.
Sugiarto, S., Persson, A.I., Munoz, E.G., Waldhuber, M., Lamagna, C., Andor, N., Hanecker, P., Ayers-Ringler, J., Phillips, J., Siu, J., et al., 2011. Asymmetry-defective oligodendrocyte progenitors are glioma precursors. Cancer Cell 20, 328–340.
Suva, M.L., Rheinbay, E., Gillespie, S.M., Patel, A.P., Wakimoto, H., Rabkin, S.D., Riggi, N., Chi, A.S., Cahill, D.P., Nahed, B.V., et al., 2014. Reconstructing and reprogramming the tumor-propagating potential of glioblastoma stem-like cells. Cell 157, 580–594.
Wegener, A., Deboux, C., Bachelin, C., Frah, M., Kerninon, C., Seilhean, D., Weider, M., Wegner, M., Nait-Oumesmar, B., 2015. Gain of Olig2 function in oligodendrocyte progenitors promotes remyelination. Brain 138, 120–135.
Wei, J., Gabrusiewicz, K., Heimberger, A., 2013. The controversial role of microglia in malignant gliomas. Clin. Dev. Immunol. 2013, 285246.
Wilson, C.B., 1992. Glioblastoma: the past, the present, and the future. Clin. Neurosurg. 38, 32–48.
Xiong, G.B., Zhang, G.N., Xiao, Y., Niu, B.Z., Qiu, H.Z., Wu, B., Lin, G.L., You, L., Shu, H., 2015. MicroRNA-219-5p functions as a tumor suppressor partially by targeting platelet-derived growth factor receptor alpha in colorectal cancer. Neoplasma 62, 855–863.
Yang, H.W., Xing, H., Johnson, M.D., 2015. A major role for microRNAs in glioblastoma cancer stem-like cells. Arch. Pharm. Res. 38, 423–434.
Yoshimura, T., 2017. The production of monocyte chemoattractant protein-1 (MCP-1)/CCL2 in tumor microenvironments. Cytokine 98, 71–78.
Young, K.M., Psachoulia, K., Tripathi, R.B., Dunn, S.J., Cossell, L., Attwell, D., Tohyama, K., Richardson, W.D., 2013. Oligodendrocyte dynamics in the healthy adult CNS: evidence for myelin remodeling. Neuron 77, 873–885.
Zhao, X., He, X., Han, X., Yu, Y., Ye, F., Chen, Y., Hoang, T., Xu, X., Mi, Q.S., Xin, M., et al., 2010. MicroRNA-mediated control of oligodendrocyte differentiation. Neuron 65, 612–626.